

# Multi-Agent Simulation of Core Spatial SIR Models for Epidemics Spread in a Population

Amelia Bădică  
University of Craiova  
Craiova, Romania  
amelia.badica@edu.ucv.ro

Costin Bădică  
University of Craiova  
Craiova, Romania  
costin.badica@edu.ucv.ro

Maria Ganzha  
Warsaw University of Technology  
Warsaw, Poland  
M.Ganzha@mini.pw.edu.pl

Mirjana Ivanović  
University of Novi Sad  
Novi Sad, Serbia  
mira@dmi.uns.ac.rs

Marcin Paprzycki  
Polish Academy of Sciences  
Warsaw, Poland  
marcin.paprzycki@ibspan.waw.pl

**Abstract**—This paper proposes a multi-agent simulation of simple core spatial Susceptible-Infected-Recovered models for epidemics spread in a population. The paper introduces the mathematical model of the system and then it proceeds by developing its multi-agent representation. The resulting multi-agent model is simulated using the GAMA multi-agent platform. The implementation and results are discussed in detail.

**Index Terms**—modeling and simulation, multi-agent system, epidemics spread

## I. INTRODUCTION

Mathematical modeling of the spreading of infectious and contagious diseases dates back to the beginning of the 20th century [1]. The goal of such models is to account for the various factors that affect the magnitude and span of the disease in a community of individuals.

One striking example that threatened humanity at the beginning of the previous century is the “1918 Flu Pandemic”, also known as the “Spanish Flu”, that lasted for more than 2 years causing death of more than 500 million people [2]. Another clearly more actual and very well-known example that the whole humanity is nowadays experiencing is the case of “Coronavirus disease 2019” or “COVID 19” contagious respiratory and vascular disease, also known as “Severe Acute Respiratory Syndrome Coronavirus 2” or “SARS-CoV-2” [3].

Agent-based modeling and simulation – ABMS is a well established modeling and simulation technique with multiple application possibilities in human systems including, among others, simulation of diffusion processes [4]. With ABMS, the designer can choose between various levels of granularity of the modelings, including macroscopic, mesoscopic and microscopic models, thus allowing him to focus on various levels of detail of the target system, as well as to trade off detail and efficiency of the modeling.

In this paper we propose a multi-agent simulation of simple spatial Susceptible-Infected-Recovered – SIR models for epidemics spread in a population. This type of models are at the core of modeling the spreading of contagious diseases in a population. The paper introduces the mathematical model of

the system and then it proceeds by developing its multi-agent representation. The resulting multi-agent model is simulated using the GAMA multi-agent platform [5]. The implementation and results are discussed in detail.

## II. BACKGROUND AND RELATED WORKS

### A. Epidemic and Related Models

Compartmental models are used in epidemiology to simplify the mathematical analysis of the spreading of infectious diseases. These models originate from the early work of Kermack and McKendrick [1]. The idea is to structure the spread of the epidemics within the population by compartments. Examples of compartments are: Susceptible, Infectious, and Recovered labeled as S, I and R. Compartmental models capture the dynamics of population transfer between compartments, according to the degree / stage of infection. Such a model can be used to study the spread of the epidemic both in time and in (geo)space.

Compartmental models can be classified according to several criteria:

- Depending on spatial and temporal characteristics of the model: temporal and spatio-temporal.
- Depending on the nature of modeling: discrete and continuous.
- Depending on model uncertainty: deterministic and stochastic.
- Depending on granularity of modeling: microscopic, mesoscopic and macroscopic.

Related models of diffusion processes were also investigated using multi-agent simulation, including agent-based emotion contagion [6], information propagation in large teams [7] and BDI models for predator-prey systems [8].

### B. Agent-Based Modeling and Simulation

Agent technologies are providing new tools and platforms for software development, modeling and simulation [9], [10], [11]. Multi-agent systems are capable to capture emergent phenomena, provide a natural description of a system and

are flexible. ABMS has been traditionally applied in the following areas of human and social systems: flow simulation, organizational simulation, market simulation, and diffusion simulation [4]. A recent survey of ABMS tools is provided by [12].

### III. MULTI-AGENT SIR MODEL

#### A. Core Spatial SIR Model

Let us consider a core spatial SIR model with the following compartments:

- $S$  compartment, here denoting the set of susceptible individuals. They are not infected. When they enter in contact with infectious individuals, they can become infected. The population of susceptible individuals at time  $t$  is denoted by  $S(t)$ .
- $I$  compartment, here denoting the set of infected individuals. They are infected and capable to infect other susceptible individuals. The population of infected individuals at time  $t$  is denoted by  $I(t)$ .
- $R$  compartment, here denoting the set of “removed” individuals. In this set we include all the individuals that either recovered, became resistant or died. The population of removed individuals at time  $t$  is denoted by  $R(t)$ .

Our model aims to capture the dynamics of individuals in space and time. Let us denote with:

$$\begin{aligned}\Delta S &= S(t + \Delta t) - S(t) \\ \Delta I &= I(t + \Delta t) - I(t) \\ \Delta R &= R(t + \Delta t) - R(t)\end{aligned}\quad (1)$$

The total population of individuals at time  $t$  is denoted with  $N(t)$  and it is defined by:

$$N(t) = S(t) + I(t) + R(t) \quad (2)$$

The spread of the disease is modeled by a factor  $F$  representing the “force of infection”. So, in each step, a fraction  $F$  of susceptible individuals from set  $S(t)$  get infected. Obviously the set  $F$  depends on the current population of susceptible individuals  $S(t)$ , as well as on the current set of infections  $I(t)$ . So the amount of susceptible individuals that get infected in the current step can be written as  $F(S(t), I(t))$ . The infected individuals will be “transferred” from the  $S$  compartment to the  $I$  compartment. It follows that:

$$\Delta S = -F(S(t), I(t)) \quad (3)$$

The specification of  $F$  depends on the model in hand. We have chosen a spatial model in which each individual has a certain physical location. Moreover, our individuals are “mobile”, i.e. they are allowed to change their location in each step. This allows us to consider the local spread of the disease in which a certain amount of individuals in the spatial vicinity of an infected individual, will get infected. Thus, “locality” of infection propagation and “mobility” of individuals enable our simple model to capture both the spatial and the temporal dimensions of the spread of the disease.

Let us denote with  $i.x$  the physical coordinate of an individual  $i$  and let  $d$  be a distance function on the space of physical locations (for example the Euclidean distance). We denote with  $V(x)$  a vicinity of  $x$ , i.e. the set of physical locations that are “close” to  $x$  according to some specific rule. One possibility is to define  $V(x)$  as the set of locations inside the ball of radius  $\epsilon$  centered at  $x$ , i.e.:

$$B(x, \epsilon) = \{y | d(x, y) \leq \epsilon\} \quad (4)$$

Let  $p \in [0, 1]$  be the probability of infection of a certain individual located in the vicinity of an infected individual. We can now easily define the selection of individuals that get infected in each step, using a stochastic selection process: for each infected individual  $i \in S(t)$  with location  $i.x$  we add to  $I(t)$  each individual  $j$  such that  $j.x \in V(i.x)$  to  $F(S(t), I(t))$  with probability  $p$ .

Let us also assume that a proportion  $\gamma \in (0, 1)$  of infected individuals (denoted in what follows with  $\gamma \cdot I(t)$ ) are removed, for example, either because they became resistant or they died. Adding also equation (3) to this system, it follows that:

$$\begin{aligned}\Delta S &= -F(S(t), I(t)) \\ \Delta I &= F(S(t), I(t)) - \gamma \cdot I(t) \\ \Delta R &= \gamma \cdot I(t)\end{aligned}\quad (5)$$

Observe that summing up equations (5) we obtain:

$$\Delta N = \Delta S + \Delta I + \Delta R = 0 \quad (6)$$

This clearly shows that for all  $t$  the total population of individuals in our model (5) does not change, i.e.:

$$N(t) = S(t) + I(t) + R(t) = \text{const.} \quad (7)$$

Note that in our model we omit the modelling of the vital aspects, i.e. the explicit birth and death of the individuals. Birth and death processes can be understood as introducing new individuals into the system and respectively discarding individuals from the system. Omitting the modeling of vital aspects can be motivated by the fact that the dynamics of the infection spread process is much faster than the usual birth and death processes and thus it can be neglected. Moreover, omitting birth and death processes can intuitively explain the conservation of the number of individuals (equation (7)).

Let us assume that on average each individual has  $\alpha$  individuals in its vicinity. However, the infection will affect only susceptible individuals from the population, so we should weight  $\alpha$  with the fraction  $\frac{S(t)}{N(t)}$  of susceptible individuals from the whole population. Then we could estimate  $F(S(t), I(t))$  as:

$$F(S(t), I(t)) = \alpha \cdot p \cdot \frac{S(t)}{N(t)} \cdot I(t) \quad (8)$$

Replacing (8) into the second equation of (5) we obtain:

$$\Delta I = \left( \frac{\alpha \cdot p}{\gamma} \cdot \frac{S(t)}{N(t)} - 1 \right) \cdot \gamma \cdot I(t) \quad (9)$$

A simple mathematical analysis of equation (9) shows that the ratio:

$$\frac{\alpha \cdot p}{\gamma} \quad (10)$$

plays a role in our model similar to the “reproduction rate” (i.e.  $R_0 = \beta/\gamma$ ) from the classical SIR model defined using differential equations (with  $\alpha \cdot p$  playing the role of parameter  $\beta$ ) [1]. The difference between the two models is however that here we indirectly control  $\beta$  by the spatial definition of what is meant by “vicinity” of an individual. For example, if we adopt the “ball model”, its radius  $\epsilon$  will determine  $\alpha$  thus indirectly controlling  $\beta$  and consequently the reproduction rate of the model.

Before concluding this section it worth mentioning that our model is “agnostic” to the underlying “topology” of the population environment. Several possibilities are envisioned including for example 2D or 3D Euclidean space, grid / lattice model, as well as arbitrary graph model.

### B. Multi-Agent Representation

The mapping of our model onto a multi-agent representation is quite straightforward. Basically, each individual becomes an agent. The compartment to which each individual is assigned is captured in our model as the agent state, one of  $S$ ,  $I$  or  $R$ . Initially most of the agents are in state  $S$ , few of them are in state  $I$ , and neither of them is in state  $R$ . At the end of the simulation, when the process stabilizes, each agent is either in state  $S$  or in state  $R$ . So state  $I$  is a “transitory state” of the agents. Moreover, if after the stabilization process all the agents are in state  $R$  it means that the epidemic reached the whole population.

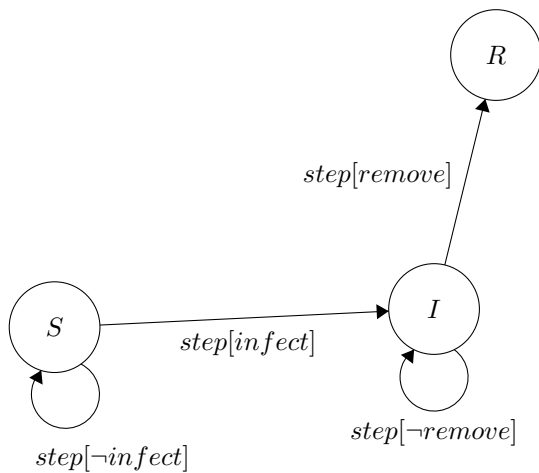


Fig. 1. State transition diagram of an individual.

The state transition diagram of each individual is modeled as a finite state automaton, as shown in Figure 1. Transitions are triggered synchronously for all the agents, at each simulation step. Note that actually state transitions are stochastic, with exact transition probabilities determined by the parameters of the system model. So in fact the behavior of our agents can be captured by a Markov chain.

Infection propagation from an agent representing an infected individual to an agent representing a susceptible individual is achieved by means of agent interaction. Basically, each

agent representing an infected individual sends an “infection message” to all the susceptible agents in its vicinity with the given probability  $p$ .

The transition of an agent from state  $I$  to state  $R$  is simply achieved by letting the agent itself update its state from  $I$  to  $R$  with probability  $\gamma$ .

Our agents are mobile, as they also model the mobility of the individuals in the population. So be design they are endowed with a spatial mobility behavior.

## IV. RESULTS AND DISCUSSION

### A. GAMA Implementation

According to [5], GAMA<sup>1</sup> “is a modeling and simulation development environment for building spatially explicit agent-based simulations.”

In GAMA, models are specifications of simulations that can be executed and controlled using experiments defined by experiment plans. Experiments facilitate the intuitive visualization of simulation results, as well as the extraction of useful simulation results.

Our implementation contains:

- The global section representing the agent environment. Here we included the definitions of all the model parameters, as well as other implementation-dependent parameters that were needed for the model visualization, like for example visual attributes used for agents visualization.
- The initialization section for setting up the initial population of agents representing the initial populations of susceptible and infected individuals.
- The class defining the agents that capture the individuals of our model, together with their internal state and behavior.
- Two sections defining our experiments for visualizing the results and extracting the simulation information. We have implemented a “gui” experiment to allow the graphical visualization and animation of the simulation, as well as a “batch” experiment for extracting simulation information as CSV files.

Each individual is modeled by an agent of *Host* species that contains the following attributes and behaviors:

- Boolean attributes *is\_susceptible*, *is\_infected*, and *is\_immune* such that at most one of them is *true*, for representing agent states  $S$ ,  $I$  and  $R$ . Initially susceptible individuals have *is\_susceptible=true* and infected individuals have *is\_infected=true*.
- Mobility is achieved by endowing our agents with *moving* skill. It defines the required actions for spatially mobile agents. In particular we have used the *wander* action for moving the agent forward to a random location at the distance computed based on its *speed* in a random direction (an angle, in degrees) determined using its *amplitude* attribute, as follows. If the current value of the direction is  $h$  and the value of the *amplitude* is  $a$  then the

<sup>1</sup><https://gama-platform.github.io/>

new value of  $h$  is chosen in the interval  $[h-a/2, h+a/2]$ . We have set  $a = 360$  to allow full coverage of all the possible directions.

- State transitions are achieved by the user-defined skills *infect* and *remove* that define the transition of an agent from state  $S$  to state  $I$  and respectively from state  $I$  to state  $R$ . The agents vulnerable for getting the infection were determined by enumerating all the agents located at a given maximum distance from an infected agent, using the *at\_distance* operator.
- Initially, our agents are randomly distributed on a square-bounded 2D space of default size  $100 \times 100$ .

Our implementation provides two basic visualizations of the simulation results:

- The spatial visualization of the agents distribution onto the 2D space. Susceptible agents are shown in green, infected agents are shown in red, while removed agents are shown in blue.
- The dynamics of susceptible, infected and removed individuals along simulation time using the same color code.

## B. Experiments and Results

Our multi-agent simulation is controlled by the following parameters that dictate the speed and magnitude of the epidemics spread in a population:

- Population size  $n$ , including initial number of susceptible individuals  $s_0$  and of infected individuals  $i_0$ . Note that  $n = s_0 + i_0$  and  $i_0 \ll s_0$ . To keep things simple and observable we have considered that  $i_0 = 2$ . This made possible to observe the epidemics spread starting from two distinct source points. Note that we kept fixed the size of our 2D space, so the population size actually dictates the population density that is expected to directly influence the spatio-temporal dynamics of the epidemics.
- The radius  $r$  of the ball defining the vicinity of an infected agent.
- The probability  $p$  that an agent in the vicinity of an infected agent will get infected; we set  $p = 0.5$  in all experiments.
- The speed  $v$  of the wandering process. Note that the angle that gives the range of the direction of the wandering process was kept constant and equal to 360 degrees.
- The proportion  $\gamma$  of infected individuals that are removed at each step; we set  $\gamma = 0.05$  in all experiments.

1) *Experiment 1*: We set  $n = 10000$ ,  $r = 1.0$  and  $v = 1.0$ . The results are shown in Figure 2. Analyzing the dynamics of population size shown in the right-hand side chart we observe that the infection reached the whole population quite fast, in approximately 140 cycles. The left-hand side figure displays the status of the population of agents during the first part of the simulation, at the 23rd cycle. We can observe how the infection progressed starting from and developing around the two source infected individuals.

2) *Experiment 2*: We set  $n = 3000$ ,  $r = 1.0$  and  $v = 1.0$ . The results are shown in Figure 3. First observe that the

density of the individuals is considerably lower than in the first experiment. The results of the population dynamics show that the process stabilized after 365 cycles with 110 susceptible individuals not reached by the epidemic. We conclude that in this scenario the epidemic progressed considerably slower than in the first experiment, and with a smaller magnitude, as it did not reach the whole population of individuals before the situation stabilized.

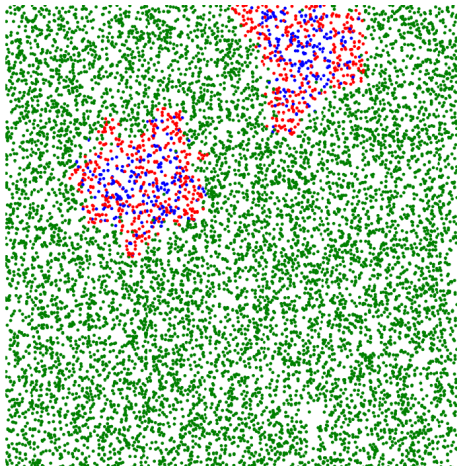
3) *Experiment 3*: We set  $n = 10000$ ,  $r = 1.0$  and  $v = 0.2$ . The results are shown in Figure 4. Comparing the results with those obtained in the first experiment, we observe that the magnitude of the epidemic spread is considerably lower (as the mobility of the individuals is lower), although the radius of the region defining the vulnerable individuals in the vicinity of an infected individual is the same. Similarly with second experiment, the epidemic did not reach the whole population before the process stabilized, leaving 537 untouched susceptible individuals. The process stabilized at the 481-th cycle.

4) *Experiment 4*: We set  $n = 10000$ ,  $r = 1.0$  and  $v = 10$ . The results are shown in Figure 5. The process stabilized somewhere after 230-th iteration leaving untouched by the infection slightly more than 1000 susceptible individuals. Analyzing the distribution of susceptible, infected and removed individuals after the 78-th iteration shown in the left-hand side of the figure, we observe that, differently from all the other experiments, individuals independently of their state tend to be much more uniformly distributed throughout the whole available space. This can be explained by the higher mobility of the individuals in this experiment, compared to experiment 1. However, comparing the magnitudes of the epidemic spread from experiments 1 and 4, it was surprising to observe that, although the mobility of agents was an order of magnitude higher in the latter case, the impact appeared to be lower (note that more than 10% of the population was not touched by the epidemic in experiment 4).

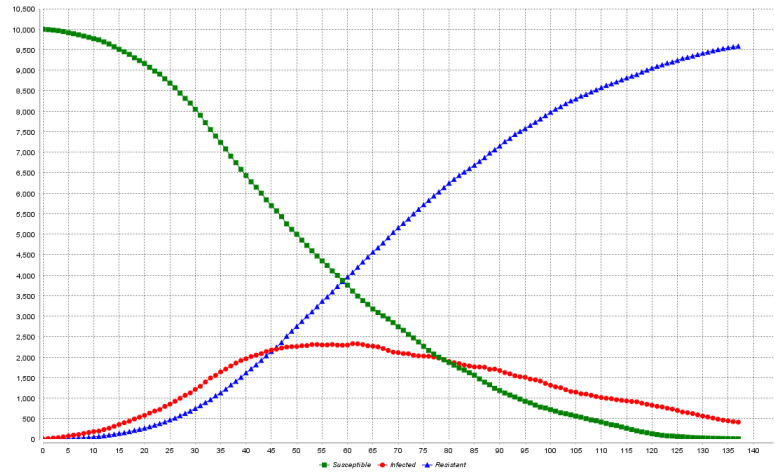
5) *Experiment 5*: We set  $n = 10000$ ,  $r = 0.3$  and  $v = 1.0$ . The results are shown in Figure 6. In this experiment the situation appears to be somehow similar with the results of experiment 3. We kept agent mobility similar to experiment 1 and decreased the impact of the spread by diminishing the radius of the region of vulnerable individuals in the vicinity of an infected individual. The process stabilized somewhere after the 60-th iteration leaving slightly more than 2000 susceptible individuals untouched by the epidemic. Comparing with the other experiments, we can conclude that in this case the magnitude of the epidemic was the lowest, leaving uninfected more than 20% of the population.

## V. CONCLUSION

We have developed a multi-agent simulation of core spatial SIR models for epidemics spread in a population using the GAMA platform. We have used the simulation system to experimentally investigate a number of scenarios. We can conclude that population density, local strength of the epidemics and mobility of the individuals strongly impact the span and magnitude of the infection spread.

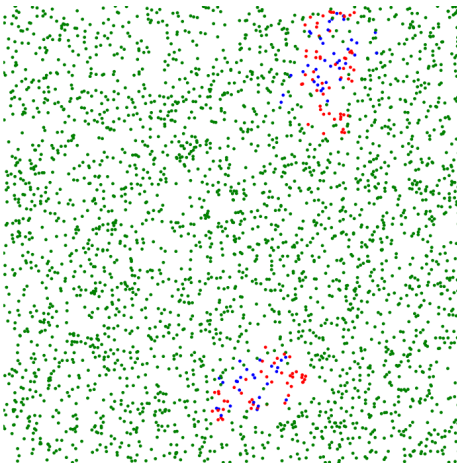


a. Population of agents after 23 cycles.

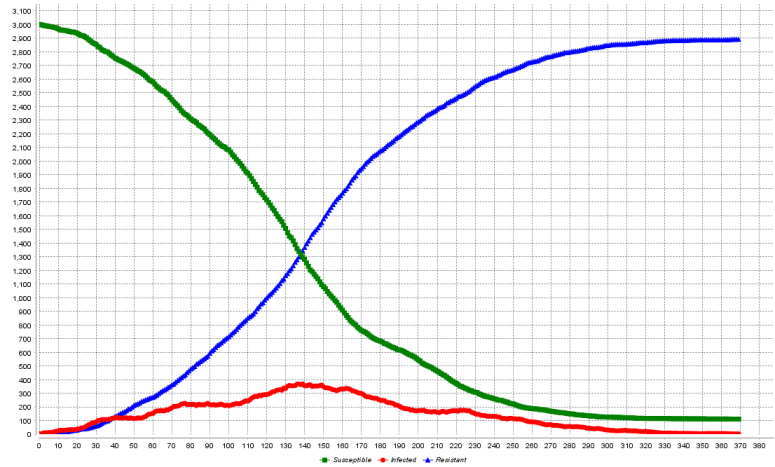


b. Dynamics of population size during 137 cycles.

Fig. 2. Results of simulation for  $n = 10000$ ,  $r = 1.0$  and  $v = 1.0$ .

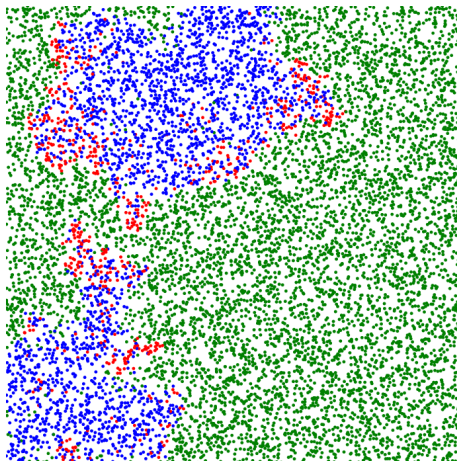


a. Population of agents after 31 cycles.

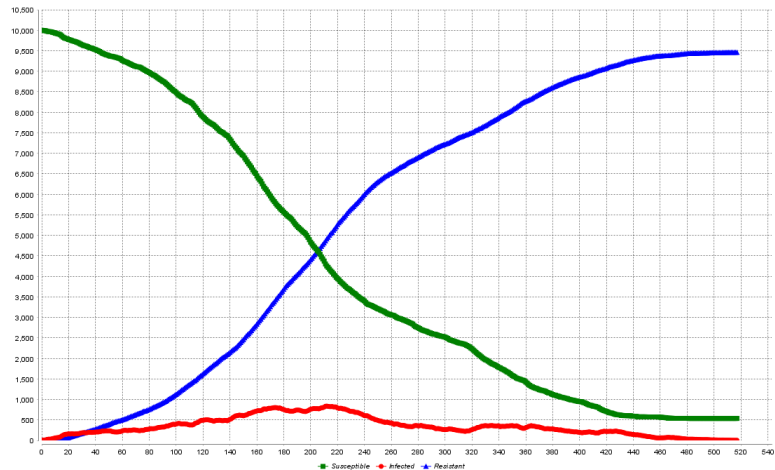


b. Dynamics of population size during 369 cycles.

Fig. 3. Results of simulation for  $n = 3000$ ,  $r = 1.0$  and  $v = 1.0$ .



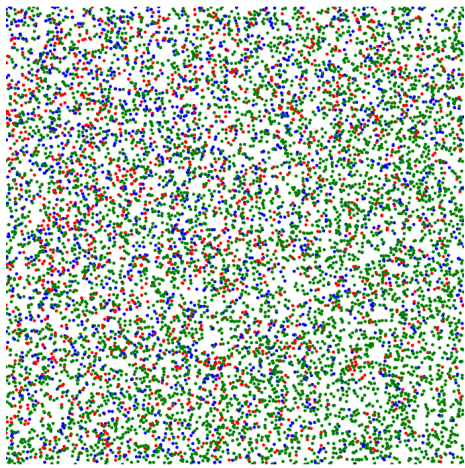
a. Population of agents after 154 cycles.



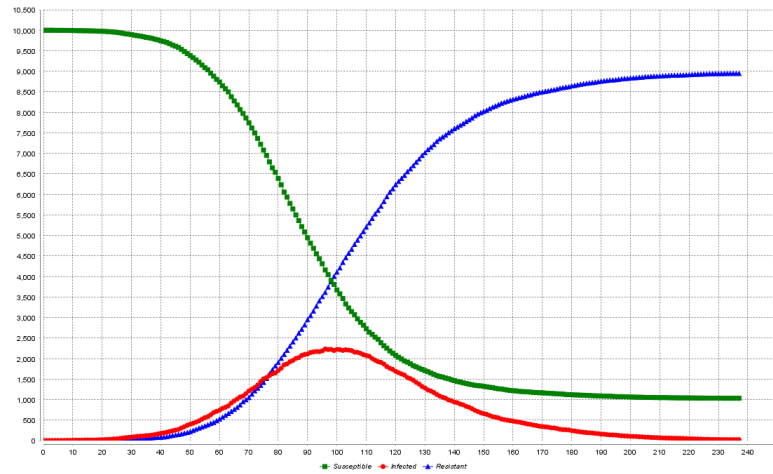
b. Dynamics of population size during 518 cycles.

Fig. 4. Results of simulation for  $n = 10000$ ,  $r = 1.0$  and  $v = 0.2$ .



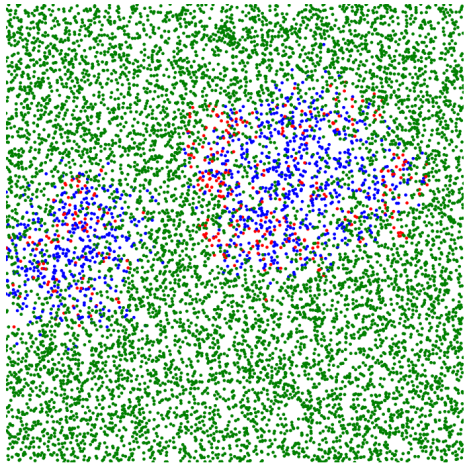


a. Population of agents after 78 cycles.

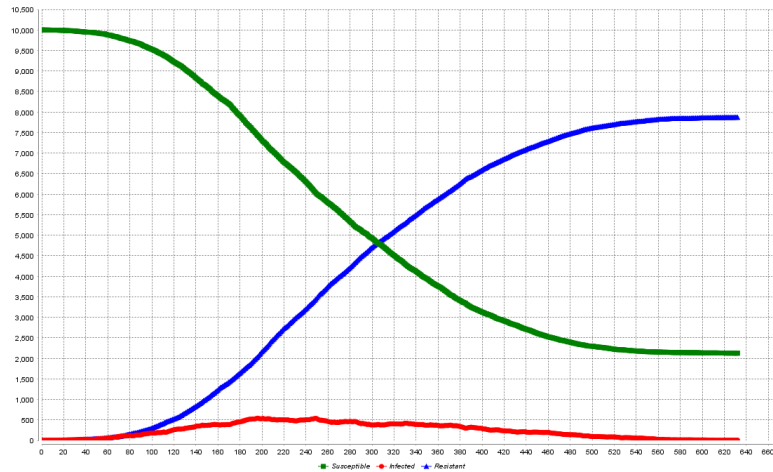


b. Dynamics of population size during 237 cycles.

Fig. 5. Results of simulation for  $n = 10000$ ,  $r = 1.0$  and  $v = 10.0$ .



a. Population of agents after 154 cycles.



b. Dynamics of population size during 632 cycles.

Fig. 6. Results of simulation for  $n = 10000$ ,  $r = 0.3$  and  $v = 1.0$ .

## REFERENCES

- [1] W. O. Kermack, A. G. McKendrick, and G. T. Walker, "A contribution to the mathematical theory of epidemics," *Proceedings of the Royal Society of London. Series A, Containing Papers of a Mathematical and Physical Character*, vol. 115, no. 772, pp. 700–721, 1927.
- [2] P. Spreeuwenberg, M. Kroneman, and J. Paget, "Reassessing the Global Mortality Burden of the 1918 Influenza Pandemic," *American Journal of Epidemiology*, vol. 187, no. 12, pp. 2561–2567, 09 2018.
- [3] R. Karia, I. Gupta, H. Khandait, A. Yadav, and A. Yadav, "Covid-19 and its modes of transmission," *SN Comprehensive Clinical Medicine*, vol. 2, no. 10, pp. 1798–1801, Oct. 2020.
- [4] E. Bonabeau, "Agent-based modeling: Methods and techniques for simulating human systems," *Proceedings of the National Academy of Sciences*, vol. 99, no. suppl 3, pp. 7280–7287, 2002.
- [5] P. Taillandier, B. Gaudou, A. Grignard, Q.-N. Huynh, N. Marilleau, P. Caillou, D. Philippon, and A. Drogoul, "Building, composing and experimenting complex spatial models with the gama platform," *GeoInformatica*, vol. 23, no. 2, pp. 299–322, 04 2019.
- [6] T. Bosse, R. Duell, Z. A. Memon, J. Treur, and C. N. van der Wal, "Agent-based modeling of emotion contagion in groups," *Cognitive Computation*, vol. 7, no. 1, pp. 111–136, 02 2015.
- [7] R. Ginton, P. Scerri, and K. Sycara, "Exploiting scale invariant dynamics for efficient information propagation in large teams," in *Proceedings of the 9th International Conference on Autonomous Agents and Multiagent Systems*, ser. AAMAS '10. Richland, SC: International Foundation for Autonomous Agents and Multiagent Systems, 2010, p. 21–30.
- [8] A. Bădică, C. Bădică, M. Ivanović, and D. Dănculescu, "Multi-agent modelling and simulation of graph-based predator-prey dynamic systems: A BDI approach," *Expert Syst. J. Knowl. Eng.*, vol. 35, no. 5, 2018.
- [9] C. Bădică, Z. Budimac, H. Burkhard, and M. Ivanović, "Software agents: Languages, tools, platforms," *Comput. Sci. Inf. Syst.*, vol. 8, no. 2, pp. 255–298, 2011.
- [10] C.-V. Pal, F. Leon, M. Paprzycki, and M. Ganzha, "A review of platforms for the development of agent systems," *arXiv.org*, 2020. [Online]. Available: <https://arxiv.org/abs/2007.08961>
- [11] K. Kravari and N. Bassiliades, "A survey of agent platforms," *Journal of Artificial Societies and Social Simulation*, vol. 18, no. 1, p. 11, jan 2015.
- [12] S. Abar, G. K. Theodoropoulos, P. Lemariniere, and G. M. O'Hare, "Agent based modelling and simulation tools: A review of the state-of-art software," *Computer Science Review*, vol. 24, pp. 13–33, 2017.